Carbohydrate Polymers 83 (2011) 926–933

Contents lists available at ScienceDirect

Carbohydrate Polymers

journal homepage: www.elsevier.com/locate/carbpol

Combined use of the free volume and coupling theories in the glass transition of polysaccharide/co-solute systems

Bin Jiang [a], Stefan Kasapis [b,*], Vassilis Kontogiorgos [c]

[a] Department of Chemistry, National University of Singapore, Science Drive 3, Singapore 117543, Singapore
[b] School of Applied Sciences, RMIT University, City Campus, Melbourne, Vic 3001, Australia
[c] Department of Chemical and Biological Sciences, The University of Huddersfield, Queensgate, HD1 3DH, UK

ARTICLE INFO

Article history:
Received 20 July 2010
Received in revised form 24 August 2010
Accepted 31 August 2010
Available online 6 September 2010

Keywords:
Free volume theory
Coupling model
Glass transition
Polysaccharide

ABSTRACT

The structural properties of the glass dispersion in agarose, κ-carrageenan and deacylated gellan with co-solute (glucose syrup) at 80.0% (w/w) solids were studied. Investigative techniques were small-deformation stress relaxation and dynamic oscillation on shear. Vitrification was monitored between −2 and −50 °C with continuous thermal runs and isothermal frequency or time sweeps obtained at constant temperature intervals. The time–temperature superposition principle was utilized to compose master curves. The Williams, Landel and Ferry equation was able to pinpoint the network T_g for these systems as the turning point from the predictions of the free volume theory in the transition region to those of the reaction rate theory at the glassy state. Further insights into the physics of intermolecular interactions at the vicinity of T_g were obtained using the coupling model of molecular dynamics in the form of the Kohlrausch, Williams and Watts function. The model described well the spectral shape of the local segmental motions in polysaccharide/co-solute samples at the short-time region of the stress–relaxation master curve. Analysis provided the intermolecular interaction constant and apparent relaxation time, which are valuable parameters for the elucidation of structural morphology at T_g.

1. Introduction

In the last 80 years or so that the scientific understanding of glassy systems has evolved, a fundamental question was the thermodynamic or kinetic nature of vitrification (Parks & Huffman, 1926). Glasses are formed when a liquid or a rubbery system is cooled so rapidly that there is no time for the molecules to rearrange themselves and pack into crystalline domains (Hutchinson, 1995). At the 'glass transition region' there is a continuity in the primary thermodynamical variables of volume, enthalpy and free energy. On the other hand, the first derivative variables of coefficient of expansion (α_p), heat capacity (C_p), etc. undergo marked changes in the course of a very few degrees (Allen, Blanshard, & Lillford, 1993). Furthermore, the spike in α_p and C_p observed at the crystallization temperature has no counterpart during vitrification. The process is considered to be in the nature of a second order thermodynamic transition in which the material undergoes a change in state but not in phase. In this context, an important consideration is the concept of plasticization and its effect on the glass transition temperature, T_g (Momany & Willett, 2002). A plasticizer is defined as a low molecular-weight substance incorporated in a material to increase its workability, flexibility or extensibility (Perry & Donald, 2002).

There is as yet no fully satisfactory theory of glass transitions but there are several valuable ways of describing them in a quantitative fashion (Montserrat, Roman, & Colomer, 2003). Synthetic science, in particular, the subject of the viscoelasticity of polymers has reached a notable level of development (Nandan, Kandpal, & Mathur, 2003), and it would make "a world of difference" if the sophisticated synthetic polymer approach could be extended to the structural conundrums of biomaterials. A certain approach used by polymer scientists to develop a mechanistic understanding of the rubber-to-glass transition is based on the concept of molecular free volume (Ferry, 1991). According to this, holes between the packing irregularities of long chain segments or the space required for their string-like movements account for free volume. Adding to that the space occupied by the van der Waals radii of polymeric contours and the thermal vibrations of individual residues, i.e. the occupied volume, we come up with the total volume per unit mass of a macromolecule. In polymer melts the proportion of free volume is usually 30% of the total volume, and the theory predicts that it collapses to about 3% at the glass transition (Cangialosi, Schut, van Veen, & Picken, 2003).

Recently, the "coupling model" has been put forward to refine analysis based on the premise that intermolecular interactions are

* Corresponding author. Tel.: +61 3 9925 5244; fax: +61 3 9925 5241.
E-mail addresses: u0203862@gmail.com (B. Jiang), stefan.kasapis@rmit.edu.au (S. Kasapis), V.Kontogiorgos@hud.ac.uk (V. Kontogiorgos).

0144-8617/$ – see front matter © 2010 Published by Elsevier Ltd.
doi:10.1016/j.carbpol.2010.08.074

more fundamental than free volume and that they are the ultimate determining factor of molecular dynamics in densely packed polymers (Ngai, 2000a). It was also felt that in order to follow structural properties within the broad glass transition region, the theory of free volume might have been unable to pinpoint the precise molecular dynamics operating at T_g (Alves, Mano, Gomez Ribelles, & Gomez Tejedor, 2004). The coupling model allows the development of a connection between the conformational chemistry of monomers and the glassy behavior of polymer, with strongly interacting systems exhibiting high values of the coupling constant, n, and an apparently broad distribution of relaxation times (Robertson & Rademacher, 2004). The parameter n need not be constant during a relaxation, hence the approach is not thermorheologically simple (TS), which is a basic assumption of the free volume theory (Robertson & Palade, 2006).

Work on polymer–solvent mixtures, polymer blends and block copolymers will provide additional tests as to the general applicability of the aforementioned framework of thought. In biomaterials, a start has been made by examining the relaxation dynamics of gelatin/co-solute mixtures throughout the glass transition region and at the vicinity of T_g (Kasapis, 2006). The present communication deals with the vitrification of polysaccharide/co-solute mixtures in conjunction with the published literature on gelatin and amorphous synthetic polymers.

2. Materials and methods

2.1. Materials

Polysaccharides agarose, κ-carrageenan, and deacylated gellan were selected for the current study due to their common gelling mechanism of coil-helix transition. Agarose (Type 1-B) was purchased from Sigma–Aldrich, Gillingham, UK. It is a material of high gel strength recorded for 2.0% (w/w) polymer concentration in aqueous preparations of a previous investigation ($G' \sim 34$ kPa at 0 °C) (Shrinivas, Kasapis, & Tongdang, 2009). Using aqueous size exclusion chromatography, the supplier determined the number average molecular weight of this agarose sample ($M_n \sim 120$ kDa). Furthermore, moisture, ash and sulfate contents were of less than 10%, 0.25% and 0.12%, respectively (w/w).

The sample of κ-carrageenan was a gift from Hercules, Lille Skensved, Denmark. ^{1}H NMR analysis showed that ι-carrageenan-like segments (i.e. with a sulfate group at position 2 of the 3,6-anhydride residue) constitute about 8% of the polymer. An Amberlite IR-120 exchanging resin from BDH was used to prepare the polysaccharide in the potassium form. κ-Carrageenan in the potassium form was characterized with intrinsic viscosity measurements, $[\eta]$, at constant ionic strength (0.01 M KCl) and 40 °C yielding $[\eta] = 10.5$ 0.2 dl/g (Kasapis & Al-Marhoobi, 2005).

The deacylated gellan sample used in this investigation was a gift from NutraSweet Kelco Company, Tadworth, UK, and it came in the sodium form. Finally, the glucose syrup used presently was a gift from Cerestar (Mechelen, Belgium). It is prepared by controlled α-(1-4)-amylase hydrolysis of wheat starch, with about 82% (w/w) amylopectin content, down to glucose sequences linked by α-(1→4) and α-(1→6) glycosidic linkages. The dextrose equivalent (DE) of the material is 42, the level of solids is 83.0% (w/w), and the water content of glucose syrup was taken into account in the calculation of the total level of solids for sample preparation.

2.2. Methods

To prepare high-solid samples, polysaccharides were dissolved in deionized water at 90 °C with stirring for 15 min and then the temperature was dropped to 70 °C for the addition of glucose syrup. A solution of calcium chloride was introduced into the sample of deacylated gellan at 70 °C to obtain 7.5 mM Ca^{2+} in the final mixture. In the case of κ-carrageenan, a solution of potassium chloride was used to obtain 10 mM K^+ in the final mixture. Excess water was evaporated off to bring the total level of solids to 80.0% (w/w). The polysaccharide content in final formulations ranged between 0.5% and 2.0% (w/w). All sample compositions mentioned below will be on w/w basis. Samples were loaded onto the preheated platen of the rheometer at 60 °C for subsequent experimentation. Throughout the temperature ramp (60 to −50 °C) they remained clear to the naked eye and adhered readily to the driving surface of the instrument. In general, the experimental temperature range was wide enough to observe a transformation from the melt to the glassy state in preparations (see, for example, Fig. 1).

Small-deformation dynamic oscillation and stress relaxation experiments on shear were used to provide readings of the storage modulus (G') which is the elastic component of the network, loss modulus (G''; viscous component), dynamic viscosity (η^*), and stress relaxation modulus, $G(t)$. Variations with time and temperature were further assessed as a measure of the 'damping factor' ($\tan\delta = G''/G'$) of the relative liquid-like and solid-like structure of the material (Malkin & Isayev, 2006). Measurements were performed with the Advanced Rheometrics Expansion System (ARES), which is a controlled strain rheometer (TA Instruments, New Castle, DE). ARES has an air-lubricated and essentially non-compliant force rebalance transducer with the torque range being between 0.02 and 2000 g cm. Parallel-plate geometry of 5 mm diameter was used and gap was kept at 1 mm.

The exposed edges of samples within the parallel-plate measuring geometry were covered with a silicone fluid from BDH (50 cS) to minimize water loss. Samples were then subjected to a controlled cooling run (scan rate: 1 °C/min) at the frequency of 1 rad/s, hence obtaining dynamic oscillatory data. Isothermal time dependence of mechanical relaxation was assessed by transient stress relaxation tests throughout the range of −50 to −2 °C at temperature intervals of 3 °C. Samples were allowed to equilibrate isothermally for 10 min following application of an instantaneous strain. This was varied from 0.02% to 1% in order to accommodate the huge changes in the measured stiffness of the sample as a function of temperature.

Three replicates were analyzed for each experimental preparation, with the rubber-to-glass transition being readily reproducible within a 3% error margin as a function of temperature or timescale of measurement. The nonlinear regression was carried out using GraphPad Prism Version 4.03.

3. Results and discussion

3.1. Dynamic oscillatory measurements as a means of observing molecular relaxations in polysaccharide/co-solute systems

The present work constitutes a demonstration of the applicability of the synthetic polymer approach to the multifarious state transitions of high-solid biomaterials. The melt-to-glass transformation of polysaccharides (or gelatin) in the presence of co-solute is of fundamental and technological interest since these systems find widespread applications in processed foods and as excipients in pharmacotherapeutics (Afoakwa, Paterson, & Fowler, 2007; Rahman, 2006). An expedient protocol to obtain information on the structural properties of these materials is to examine the variation in G' and G' traces as a function of temperature at a constant frequency or time of observation. This is illustrated in Fig. 1(a–c) for typical preparations of agarose, κ-carrageenan and deacylated gellan in the presence of glucose syrup as the co-solute, with the total level of solids in each case being adjusted to 80.0%.

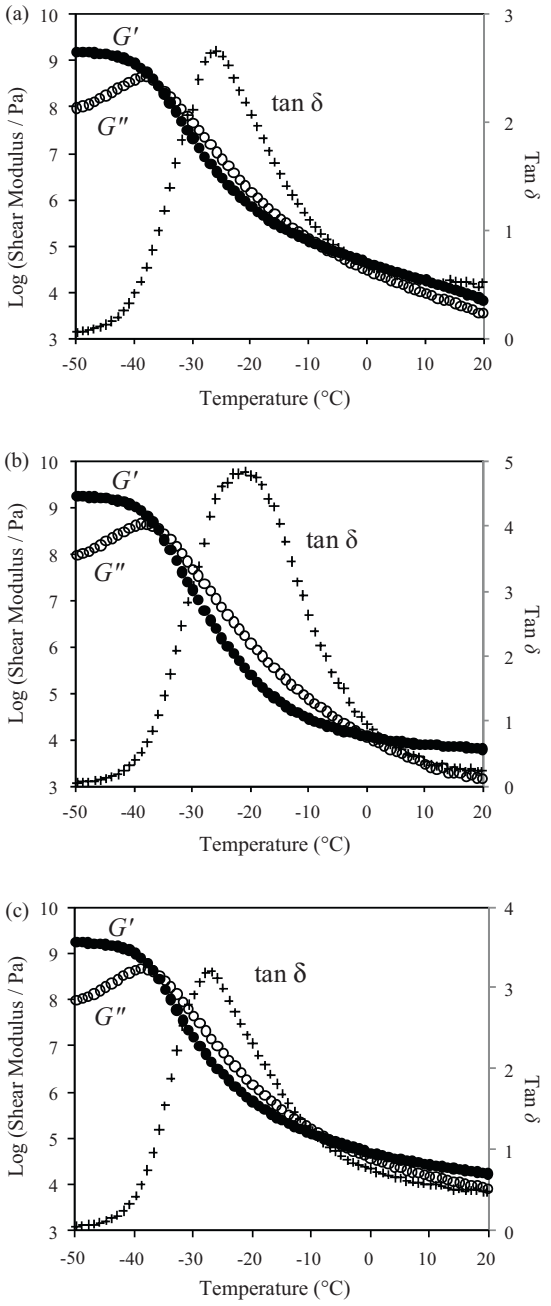

Fig. 1. Temperature dependence of G', G'' and tan δ for (a) 2.0% agarose plus 78.0% glucose syrup, (b) 0.5% κ-carrageenan plus 79.5% glucose syrup at 10 mM added KCl and (c) 1.0% deacylated gellan plus 79.0% glucose syrup at 7.5 mM added $CaCl_2$ (scan rate: 1 °C/min; frequency: 1 rad/s; strain: 0.01–1.0%).

Considerable part of the "master curve of viscoelasticity" has been captured within the experimentally accessible temperature that ranged between 20 and −50 °C. In detail, the contribution of polymeric network to viscoelastic behavior is seen at the upper range of temperatures where the storage modulus dominates the loss modulus leading to the formation of rubbery systems. Values of G' and G'' remain relatively flat between 0 and 20 °C at about 10^4 Pa. In the rubbery region, these are "true" gels that can support their shape against gravity at ambient temperature and undergo a coil-to-helix transition at higher temperatures as monitored by dynamic oscillatory and differential scanning calorimetry profiles at high temperatures (50–40 °C; results are not shown here).

On further cooling (i.e. below 0 °C in Fig. 1), the shear moduli develop rapidly and we consider values up to 10^8 Pa. This is the glass transition region where a notable observation is the spectacular development of viscoelasticity, in this case, four orders of magnitude from ~10^4 to 10^8 Pa. In addition, viscoelastic parameters cross over and make the viscous component of the network dominant ($G'' > G'$) hence indicating that extensive topological entanglement or non-covalent cross-linking, which governs mechanical response in the rubbery plateau, is not of overriding importance in this region (Tsui, Paraskos, Torun, Swager, & Thomas, 2006). Long range movements of the main chain contributing to elasticity are restricted but local relaxation processes that dissipate energy, for example of pendant groups, can occur leading to viscous outputs (Kasapis, Sablani, Rahman, Al-Marhoobi, & Al-Amri, 2007).

At the lowest range of temperatures below −40 °C, there is yet another development, with modulus traces crossing over for a second time ($G' > Gc'$) resulting in a hard-solid response. This is the fourth region of the master curve of viscoelasticity, the so-called glassy state where transverse string-like vibrations of polymeric chains diminish with reduced temperature (Rahman, Al-Marhubi, & Al-Mahrouqi, 2007). Stretching and bending of chemical bonds and other secondary mechanisms, for example of local segmental motions, are ubiquitous here leading to a dominant elastic output (Jazouli, Luo, Bremand, & Vu-Khanh, 2005). In the glassy stage depicted in Fig. 1, the storage modulus is increasingly dominant and approaches equilibrium values in excess of 10^9 Pa, whereas the values of loss modulus diminish rapidly and end below 10^8 Pa in the recorded spectrum. All along, the derived damping factor ($\tan \delta = G''/G'$) exhibits associated changes of peak maxima, which are well above the value of one, in the glass transition region followed by large drops in magnitude in the glassy state (near zero at −50 °C).

3.2. Utilization of the time–temperature superposition principle as a means of modeling the relaxation behavior of polysaccharide/co-solute systems

The thermal profiles of small-deformation modulus discussed in Fig. 1 allow a first insight into the structural properties of our materials. Measurements involve relaxation processes can be analyzed mathematically in terms of the mechanical spectrum of relaxation times (Shivakumar, Das, Segal, & Narkis, 2005). This information is more valuable, it allows complete dissociation of the contributions of temperature and frequency to the overall mechanical behavior according to the postulates of the time–temperature superposition (TTS). TTS affords a device for changes in temperature to be seen as shifts in the frequency or time scale of mechanical spectra taken in a sequence of temperature intervals (Hrma, 2008).

This work implemented TTS with oscillatory frequency sweeps at fixed temperature intervals covering the range of −2 to −50 °C. In addition, it pursued the same exercise by implementing a series of time runs and monitoring the decay of stress–relaxation modulus, $G(t)$, over time. In the following, we opted to show data of the modulus $G(t)$ in order to expedite derivation of relaxation parameters that require use of the Kohlrausch, Williams and Watts (KWW) function (Hahn & Hillmyer, 2003). Numerical techniques are available to obtain $G(t)$ from $G'(\omega)$ and $G''(\omega)$ but the Fourier transforms involved may discourage workers from doing so (Plazek, Chay, Ngai, & Roland, 1995).

Fig. 2(a–c) reproduces data of the stress–relaxation modulus, which were recorded for mixtures of agarose, κ-carrageenan and deacylated gellan with glucose for seventeen different temperatures. Traces covering the long timescales of the upper range of temperature remain relatively flat within the rubbery region (e.g. at −2 °C). Further cooling sees a rapid reinforcement of mechanical response shaping up an exponential profile that follows the glass transition region (e.g. at −26 °C). At the low-temperature end of the present experimental range, the values of $G(t)$ level off once

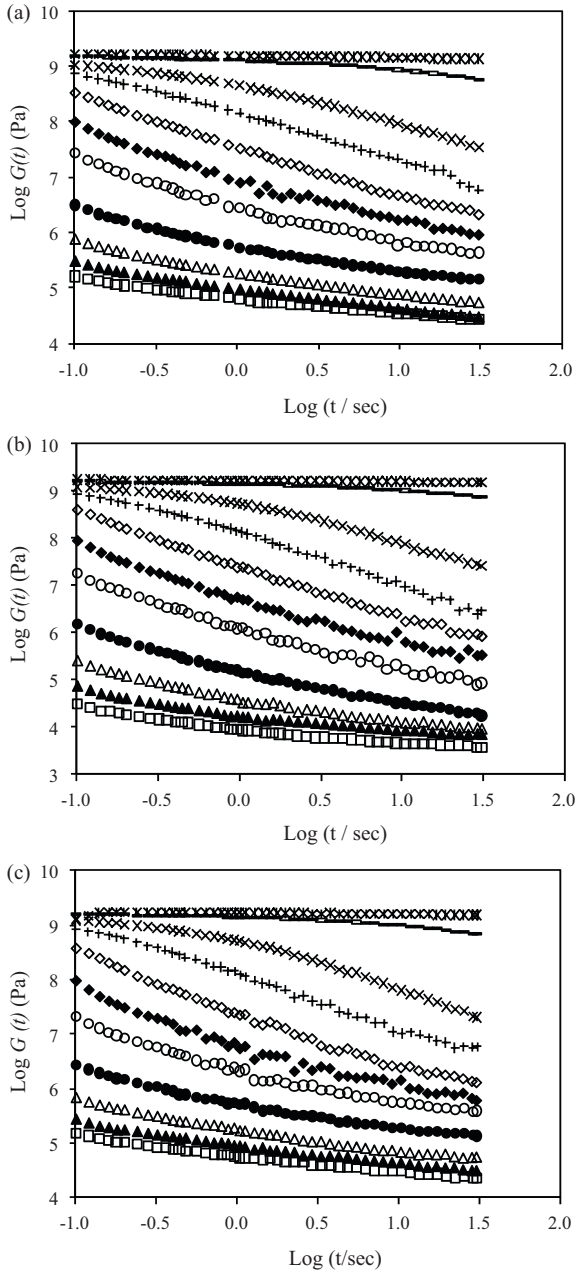

Fig. 2. Variation of the stress relaxation modulus at fixed temperatures for the following samples: (a) 2.0% agarose plus 78.0% glucose syrup, (b) 0.5% κ-carrageenan plus 79.5% glucose syrup at 10 mM added KCl and (c) 1.0% deacylated gellan plus 79.0% glucose syrup at 7.5 mM added $CaCl_2$. Bottom curve is taken at −2 °C (□); other curves successively upward: −8 (▲); −14 (△); −20 (●); −26 (○); −29 (♦); −32 (◊); −35 (+); −38 (×); −44 (–); −50 (*) °C. Stress relaxation curves at −5, −11, −17, −23, −41, and −47 °C are not plotted to avoid clutter.

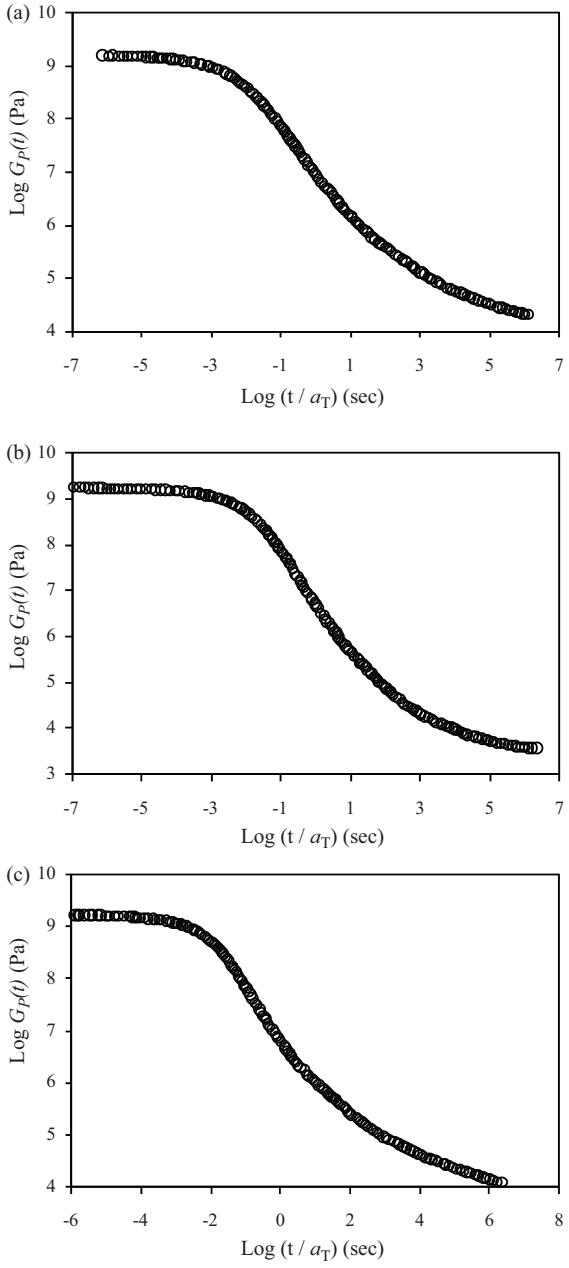

Fig. 3. Master curve of stress relaxation modulus for the following samples: (a) 2.0% agarose plus 78.0% glucose syrup, (b) 0.5% κ-carrageenan plus 79.5% glucose syrup at 10 mM added KCl and (c) 1.0% deacylated gellan plus 79.0% glucose syrup at 7.5 mM added $CaCl_2$. Data were reduced to −29 °C and plotted logarithmically against logarithmic reduced time (t/a_T) utilizing the experimental isothermal runs of Fig. 2.

more with a quantifiable end-point thus unveiling the glassy state at −50 °C.

Further inroads into this school of thought require data reduction to a standard temperature that should lie within the glass transition region. This is fulfilled presently by choosing arbitrarily −29 °C as the reference temperature (T_0) and shifting the remaining mechanical spectra left and right of this focal point along the log time axis. In doing so, the viscoelasticity at any stage of the thermal run can be related to that of the reference temperature as long as the timescale of the former is divided by a shift factor, a_T, that reflects the extent of shifting (Huang & Paul, 2004). Exact matching of the shape of adjacent curves is a prerequisite for the applicability of TTS (Li & Yee, 2003). The factor a_T was determined by the software of ARES (TA Orchestrator 7.0) which minimizes the error, i.e. the average of the sum of the local residuals. Each local residual is the norm (vector length) between two data points: one lying along the curve that was shifted and the other along the curve to which it was shifted. Values were also reproduced manually by measuring the horizontal distance between each pair of adjacent curves with a pair of dividers and recording as $\Delta \log a_T$.

Fig. 3(a–c) depicts the outcome of the horizontal superposition of the isothermal data discussed in Fig. 2 at the reference temperature of −29 °C. This creates master curves of stress relaxation for the three polysaccharide/co-solute systems, with the reduced variable $G_p(t)$ being plotted logarithmically. The composite spectrum is

a sigmoidal curve that extends over twelve orders of magnitude in timescale hence showing the transformation from a rubbery state at long times (>10^4 s) to a glassy state at short times (<10^{-3} s). Between the two extrema, modulus values rise rapidly in the glass transition and shape up the time analogue of the experimental temperature ramp recorded in Fig. 1.

3.3. Parameterization of the composite curve of stress relaxation modulus in high-solid polysaccharide/co-solute systems

To move from the qualitative description of vitrification phenomena described in the preceding sections, we take advantage of the shift factor, a_T, which was used in the reduction of mechanical spectra in Fig. 3. The main objective of this part of analysis is to pinpoint the glass transition temperature (T_g) of various preparations and this can be expedited by utilizing the concept of molecular free volume. The approach is compatible with the equation proposed by Williams, Landel and Ferry (WLF), which for the stress relaxation modulus recasts in the following mathematical form (Ferry, 1980):

$$\log a_T = \log\left[\frac{G(t)(T)}{G(t)T_0}\right] = -\frac{B(T-T_0)/2.303f_0}{f_0/a_f + T - T_0} \quad (1)$$

where, the fractional free volume, f_0, is the ratio of free to total volume of the molecule, α_f is the thermal expansion coefficient, and B is usually set to one. The terms $B/2.303f_0$ and f_0/α_f are known as the WLF parameters C_1^0 and C_2^0, respectively.

Application of the combined framework of WLF/free volume theory to the three sets of horizontal shift factors of the polysaccharide/co-solute systems is depicted in Fig. 4(a–c). Eq. (1) provides a good fit of the empirically derived shift factors in the glass transition region, which, for example, extends from about −2 to −35 °C for the κ-carrageenan preparations. This outcome argues that free volume is the molecular mechanism dictating diffusional mobility within this temperature range.

As shown in Fig. 4, however, the shift factors of stress relaxation spectra at lower temperatures (<−40 °C) unveil a pattern of behavior that cannot be followed by the WLF equation. Instead, progress in mechanical properties in this region is better described by the modified Arrhenius equation (Kasapis, 2008):

$$\log a_T = \frac{E_a(1/T - 1/T_0)}{2.303R} \quad (2)$$

This yields the concept of activation energy (E_a) for an elementary flow process, which is independent of temperature. It appears, therefore, that within the glassy state the factor a_T is an exponential function of the reciprocal absolute temperature, so the logarithmic form with a constant energy of activation for an elementary flow process can be used for calculating numerical values.

Clearly, the analysis amounts to more than curve fitting since it identifies in Fig. 4 the glass transition temperature of preparations as a turning point where large configurational vibrations requiring free volume cease to be of overriding importance. Free volume parameters produced from the temperature dependence of shift factor for the stress–relaxation data of our polysaccharide/glucose syrup mixtures are given in Table 1. This definition of T_g at the threshold of predictions of free volume and reaction rate theories appears to be an improvement on several empirical indices of the mechanical T_g, which recorded an array of discontinuities in the slope of storage or loss modulus traces and large peaks in the damping factor, tan δ (Rieger, 2001; Kasapis, Al-Marhoobi, & Mitchell, 2003). In the absence of a fundamental criterion, however, it seems barely credible to pinpoint glassy phenomena, or any other molecular events (thermal relaxation, molecular degradation, etc.) to empirical indices of pictorial rheology.

At this juncture, we also note an underlying process that becomes increasingly apparent in the literature. This relates to

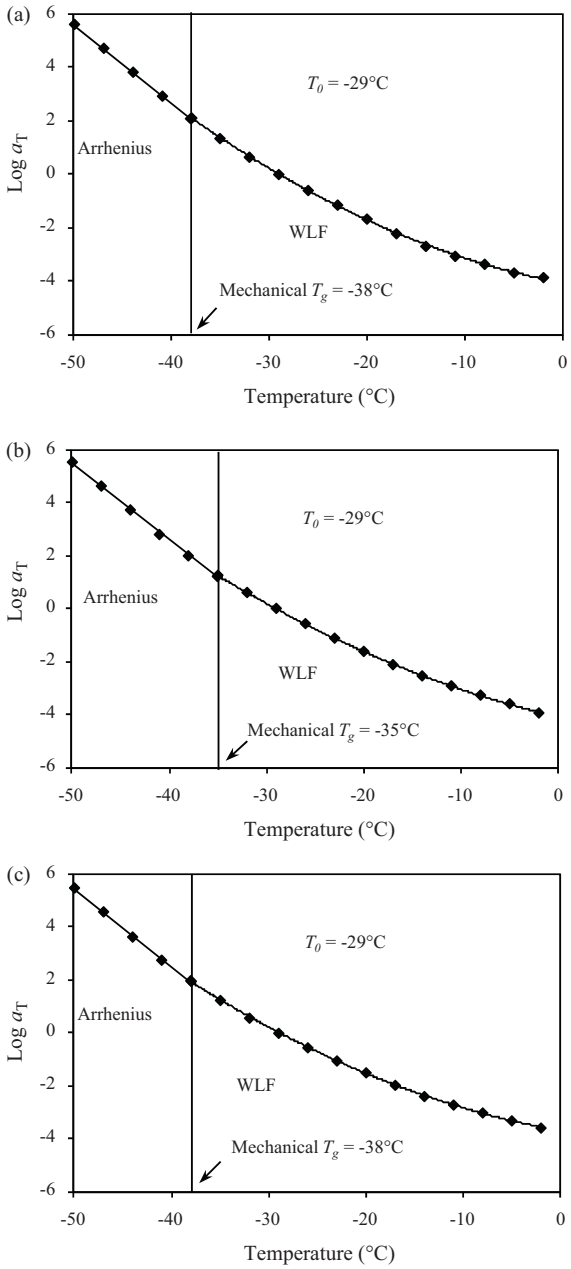

Fig. 4. Logarithm of the reduction factor, a_T, for samples: (a) 2.0% agarose plus 78.0% glucose syrup, (b) 0.5% κ-carrageenan plus 79.5% glucose syrup at 10 mM added KCl and (c) 1.0% deacylated gellan plus 79.0% glucose syrup at 7.5 mM added $CaCl_2$, plotted against temperature from the data of the master curves in Fig. 3. Reference temperature, mechanistic modeling and the mechanical glass transition temperatures are also shown.

the observation that besides a thorough description of the material in terms of its composition or preparation history, the glass transition temperature depends on the analytical method and protocol employed (Schmidt, Belton, Hills, & Webb, 1999; Schmidt, 2004). Glass transition temperatures obtained for 80.0% (w/w) glucose syrup by differential scanning calorimetry are close to −44.0 °C (results are not shown here), whereas in the presence of gelling polysaccharide values of the mechanical T_g are higher about 9 °C (Fig. 4). Unlike the DSC T_g, the mechanical T_g is affected by the nature of the macromolecule and cannot be predicted by the basic theoretical frameworks for mixed systems such as the Couchman–Karasz equation (Couchman & Karasz, 1978). The apparent acceleration of vitrification is related to the ability of

Table 1
Parameterization derived from the WLF/free volume and KWW/coupling model theories for the structural properties of polysaccharide/co-solute systems at glass transition.

Polysaccharide/glucose syrup	C_1^0	C_2^0 (°)	f_0	$C_1{}^g$	$C_2{}^g$ (°)	f_g	αf ($\times 10^{-4}$ °C^{-1})	T_g (°C)	n	τ (s)
Agarose	15.5	74.0	0.028	17.6	65.0	0.025	3.8	−38.0	0.64	0.186
κ-Carrageenan	14.9	74.3	0.029	16.2	68.3	0.027	3.9	−35.0	0.60	0.047
Deacylated gellan	12.4	64.9	0.035	14.4	55.9	0.030	5.4	−38.0	0.59	0.290

polysaccharide to form a network, thus making the mechanical T_g synonymous to a network T_g. Therefore, the discrepancies observed in the values of mechanical and DSC T_g should not be perceived as an experimental artifact but, rather, a reflection of the distinct property and different scale being probed by the two techniques.

Once the mechanical T_g is pinpointed, the stage is set for a more explicit analysis that considers the strength of interactions of local segmental motions responsible for the completion of vitrification with decreasing temperature. This type of information is not forthcoming from the WLF/free volume approach, which aims to follow the development of structural properties within the entirety of the broad glass transition region. At the glass transition temperature, Gaussian submolecular motions of the extended Rouse model should contribute minimally to the viscoelastic spectrum allowing the local segmental motions to dominate (Tchesskaya, 2005). The nature of the local segmental motions is responsible for the glass transition temperature of an individual system, as monitored using several well established techniques (Roland & Ngai, 1991). In particular, the extent of interactions between neighboring segments relates to the distribution of relaxation times and can be followed by the so-called stretched exponential function of Kohlrausch, Williams and Watts (KWW) in the time domain (Ngai, 2000b):

$$\phi(t) = \exp\left[-\left(\frac{t}{\tau}\right)\right]^{\beta} \quad (3)$$

where $\phi(t)$ and τ are the relaxation function and time, respectively. The stretch exponent β can take values between 0 and 1.0 thus imparting a non-exponential character to the kinetics of structural relaxation of glassy materials. At the times appropriate for mechanical measurements, Eq. (3) recasts for the stress relaxation modulus of the present investigation as follows (Ngai, Magill, & Plazek, 2000):

$$G(t) = (G_g - G_e)\exp\left[-\left(\frac{t}{\tau}\right)\right]^{1-n} + G_e \quad (4)$$

where, G_g is the unrelaxed glassy modulus, G_e is the relaxed or equilibrium modulus of the local segmental motions and t is the time after the application of a fixed strain. The coupling constant, n ($\beta = 1 - n$), ranges from 0 to 1.0, reflects the intensity of interactions (coupling) between the primitive (underlying) relaxation and the physicochemical environment of the surrounding materials.

Eq. (4) has been designed to follow relaxation patterns reflecting segmental mobility provided that experimental values of the decaying stress–relaxation modulus fall within the range of $G_g > G(t) > G_e$. Secondary (β) relaxations would be responsible for the region $G(t) > G_g$, whereas extended Rouse-like modes are expected to dominate at $G(t) < G_e$. Appropriate values of the unrelaxed and equilibrium modulus were selected for each preparation (e.g. G_g and G_e are taken to be about 1.8×10^9 and 0.3×10^9 Pa, respectively, for the agarose/co-solute sample). This is in accordance with experience from synthetic polymer research where the modulus ratio (G_g/G_e) is within an order of magnitude (Ngai & Yee, 1991).

Fig. 5(a–c) reproduces parts of the stress–relaxation composite curves of the polysaccharide/co-solute samples, which constitute the extreme short-time segments of the rubber-to-glass transition. Materials were tailored made at 80% total solids and specific polysaccharide concentrations to produce similar glass transition temperatures (−35 to −38 °C). Data fits were implemented at the glass transition temperature of each preparation by fitting $G(t)$ versus t with the two-parameter KWW function of Eq. (4), thus obtaining n and τ, with the regression coefficient and regression

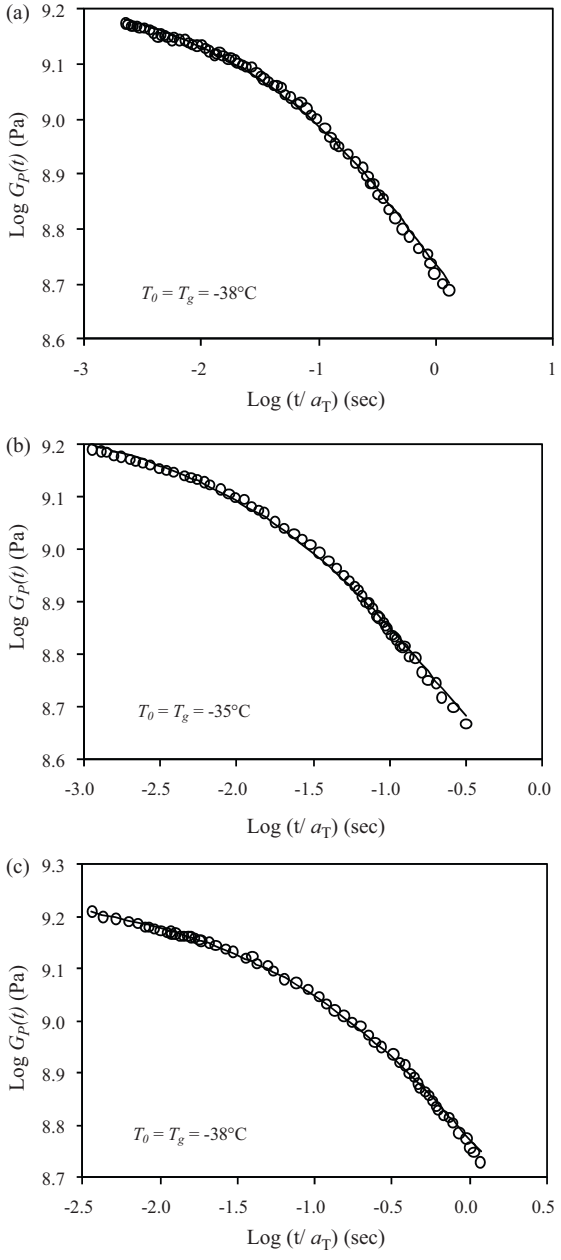

Fig. 5. Short-time region of the stress–relaxation master curve for samples (a) 2.0% agarose plus 78.0% glucose syrup, (b) 0.5% κ-carrageenan plus 79.5% glucose syrup at 10 mM added KCl and (c) 1.0% deacylated gellan plus 79.0% glucose syrup at 7.5 mM added $CaCl_2$, using their respective T_gs as reference temperature, with open circles and solid lines indicating experimental data and the predictions of the KWW function, respectively.

loss of the estimated functions being 0.996–0.999 and 0.018–0.020, respectively.

In Fig. 5, KWW modeling follows well the progression of mechanical data yielding values of the coupling constant and relaxation time for our materials, which are reproduced in Table 1. According to work in amorphous synthetic polymers, the higher the value of n the stronger the intermolecular coupling, which originates from the chemical structure of the macromolecule and its surrounding environment. It was found that the n values of strongly interlinking or sterically interfering chains of synthetic materials range between 0.66 and 0.77 (poly(vinyl chloride), poly(methylmethacrylate), etc.) (Ngai & Plazek, 1995). Earlier work on gelatin/glucose syrup mixtures produced a coupling-constant estimate of 0.57. That was a reasonable finding considering that gelatin forms a non-aggregating network and a decrease in the surface of contact between the protein and polyhydroxyl co-solute is necessary to induce thermodynamically favorable conditions in the mixture (Kasapis, 2006).

Polysaccharides, on the other hand, exhibit distinct topology from that of gelatin in mixture with small polyhydroxyl compounds, with their network effectively being dissolved in the saturated co-solute environment (Kasapis, Al-Marhoobi, Deszczynski, Mitchell, & Abeysekera, 2003; Kasapis, Al-Marhoobi, & Mitchell, 2003). This should generate strong interactions between neighboring segments reflected in the values of coupling constant that extend to 0.64 in the case of agarose. As argued, the preferential exclusion of co-solute from the domain of gelatin prohibits the formation of a solvation sheath around the protein, which also results in a rapid relaxation time ($\tau \approx 0.2 \times 10^{-4}$ s). In support to the argument developed presently, molecular interactions between polysaccharide segments and glucose syrup are also seen in relatively high values of the apparent relaxation time of local segmental motions, i.e., τ is ~0.047 s for the example of κ-carrageenan at the glass transition temperature.

4. Conclusions

In the past few years, there has been vigorous debate regarding the most appropriate school of thought for the treatment of structural properties of glassy biomaterials. The prevalent analytical framework traditionally employed to follow the transition from rubbery to glasslike consistency in these systems is that of the free volume theory in conjunction with the WLF equation. Increasingly, this approach is challenged in synthetic polymer research by the coupling model/Kohlrausch–Williams–Watts function which is able to focus on the physics of intermolecular interactions at the vicinity of the glass transition temperature. The purpose of the present communication is to demonstrate that the atmosphere of exclusivity of one theory or rejection of the second one is not justified, with both approaches being complementary in the description of the many-body dynamics recorded during vitrification of biomaterials. Thus, the free volume theory described by the WLF equation was used to identify the mechanical T_g of agarose, κ-carrageenan, deacylated gellan and co-solute at 80% total solids as a threshold of physical significance based on the predictions of the free volume and reaction rate theories.

In contrast, an arbitrary predetermined relaxation time was used in certain studies that dealt with the application of the coupling model to the structural behaviour of amorphous and semicrystalline synthetics, and this has been taken to be 100 s so that $T_g = T(\langle\tau\rangle = 100\,\text{s})$. It has been documented in the literature, however, that the relaxation map of both types of materials exhibits considerable temperature dependence, and there is no fundamental basis in relating $\tau(T_g) = 100$ s or any hypothetical indicator of a long relaxation time to a glass point. The present work circumvents the condition that makes the local segmental motions of various materials to associate with the same and arbitrary relaxation time by building on the temperature dependence of factor a_T shown in Fig. 4(a–c). This temperature dependence exhibits a discontinuity, which remains unaltered and pinpoints the glass transition temperatures in the present systems.

By relating the mechanical T_g to local segmental motion, valid application of the coupling theory in conjunction with the KWW function can be implemented yielding the coupling constant and relaxation time in polysaccharide/glucose syrup glasses. These parameters relate to specifics of chemical structure and as such were contrasted with molecular dynamics of other densely packed systems at the glass transition region (amorphous synthetics and gelatin/co-solute). A clear pathway has thus been developed that relates fundamentals of the theory of glass transition to strongly interlinking, sterically interfering, non-aggregating/dissolving and phase separating macromolecules in a high solid environment.

References

Afoakwa, E. O., Paterson, A., & Fowler, M. (2007). Factors influencing rheological and textural qualities in chocolate—a review. *Trends in Food Science & Technology*, *18*, 290–298.

Allen, G., Blanshard, J. M. V., & Lillford, P. J. (1993). *The glassy state in foods*. Nottingham: University Press., pp. 1–12.

Alves, N. M., Mano, J. F., Gomez Ribelles, J. L., & Gomez Tejedor, J. A. (2004). Departure from the Vogel behaviour in the glass transition—thermally stimulated recovery, creep and dynamic mechanical analysis studies. *Polymer*, *45*, 1007–1017.

Cangialosi, D., Schut, H., van Veen, A., & Picken, S. J. (2003). Positron annihilation lifetime spectroscopy for measuring free volume during physical aging of polycarbonate. *Macromolecules*, *36*, 142–147.

Couchman, P. R., & Karasz, F. E. (1978). A classical thermodynamic discussion of the effect of composition on glass-transition temperatures. *Macromolecules*, *11*, 117–119.

Ferry, J. D. (1980). *Viscoelastic properties of polymers*. New York: John Wiley., pp. 264–320.

Ferry, J. D. (1991). Some reflections on the early development of polymer dynamics: Viscoelasticity, dielectric dispersion, and self-diffusion. *Macromolecules*, *24*, 5237–5245.

Hahn, S. F., & Hillmyer, M. A. (2003). High glass transition temperature polyolefins obtained by the catalytic hydrogenation of polyindene. *Macromolecules*, *36*, 71–76.

Hrma, P. (2008). Arrhenius model for high-temperature glass-viscosity with a constant pre-exponential factor. *Journal of Non-Crystalline Solids*, *354*, 1962–1968.

Huang, Y., & Paul, D. R. (2004). Physical aging of thin glassy polymer films monitored by gas permeability. *Polymer*, *45*, 8377–8393.

Hutchinson, J. M. (1995). Physical aging of polymers. *Progress in Polymer Science*, *20*, 703–760.

Jazouli, S., Luo, W., Bremand, F., & Vu-Khanh, T. (2005). Application of time–stress equivalence to nonlinear creep of polycarbonate. *Polymer Testing*, *24*, 463–467.

Kasapis, S. (2006). Building on the WLF/free volume framework: Utilization of the coupling model in the relaxation dynamics of the gelatin/cosolute system. *Biomacromolecules*, *7*, 1671–1678.

Kasapis, S. (2008). Recent advances and future challenges in the explanation and exploitation of the network glass transition of high sugar/biopolymer mixtures. *Critical Reviews in Food Science and Nutrition*, *48*, 185–203.

Kasapis, S., & Al-Marhoobi, I. M. (2005). Bridging the divide between the high- and low-solid analysis in the gelatin/κ-carrageenan mixture. *Biomacromolecules*, *6*, 14–23.

Kasapis, S., Al-Marhoobi, I. M., Deszczynski, M., Mitchell, J. R., & Abeysekera, R. (2003). Gelatin vs polysaccharide in mixture with sugar. *Biomacromolecules*, *4*, 1142–1149.

Kasapis, S., Al-Marhoobi, I. M., & Mitchell, J. R. (2003). Testing the validity of comparisons between the rheological and the calorimetric glass transition temperatures. *Carbohydrate Research*, *338*, 787–794.

Kasapis, S., Sablani, S. S., Rahman, M. S., Al-Marhoobi, I. M., & Al-Amri, I. S. (2007). Porosity and the effect of structural changes on the mechanical glass transition temperature. *Journal of Agricultural and Food Chemistry*, *55*, 2459–2466.

Li, X., & Yee, A. F. (2003). Design of mechanically robust high-T_g polymers: Synthesis and dynamic mechanical relaxation behavior of glassy poly(ester carbonate)s with cyclohexylene rings in the backbone. *Macromolecules*, *36*, 9411–9420.

Malkin, A. Ya., & Isayev, A. I. (2006). *Rheology—concepts, methods & applications*. Toronto: ChemTec Publishing.

Momany, F. A., & Willett, J. L. (2002). Molecular dynamics calculations on amylose fragments. I. Glass transition temperatures of maltodecaose at 1, 5, 10, and 15.8% hydration. *Biopolymers*, *63*, 99–110.

Montserrat, S., Roman, F., & Colomer, P. (2003). Vitrification and dielectric relaxation during the isothermal curing of an epoxy-amine resin. *Polymer*, *44*, 101–114.

Nandan, B., Kandpal, L. D., & Mathur, G. N. (2003). Glass transition behaviour of poly(ether ether ketone)/poly(aryl ether sulphone) blends: Dynamic mechanical and dielectric relaxation studies. *Polymer*, *44*, 1267–1279.

Ngai, K. L. (2000a). Short-time and long-time relaxation dynamics of glass-forming substances: A coupling model perspective. *Journal of Physics: Condensed Matter*, *12*, 6437–6451.

Ngai, K. L. (2000b). Dynamic and thermodynamic properties of glass-forming substances. *Journal of Non-Crystalline Solids*, *275*, 7–51.

Ngai, K. L., Magill, J. H., & Plazek, D. J. (2000). Flow, diffusion and crystallization of supercooled liquids: Revisited. *Journal of Chemical Physics*, *112*, 1887–1892.

Ngai, K. L., & Plazek, D. J. (1995). Identification of different modes of molecular motion in polymers that cause thermorheological complexity. *Rubber Chemistry and Technology*, *68*, 376–434.

Ngai, K. L., & Yee, A. F. (1991). Some connections between viscoelastic properties of PVC and plasticized PVC and molecular kinetics. *Journal of Polymer Science: Part B: Polymer Physics*, *29*, 1493–1501.

Parks, G. S., & Huffman, H. M. (1926). Glass as a fourth state of matter. *Science*, *64*, 363–364.

Perry, P. A., & Donald, A. M. (2002). The effect of sugars on the gelatinisation of starch. *Carbohydrate Polymers*, *49*, 155–165.

Plazek, D. J., Chay, I.-C., Ngai, K. L., & Roland, C. M. (1995). Viscoelastic properties of polymers. 4. Thermorheological complexity of the softening dispersion in polyisobutylene. *Macromolecules*, *28*, 6432–6436.

Rahman, M. S. (2006). State diagram of foods: Its potential use in food processing and product stability. *Trends in Food Science & Technology*, *17*, 129–141.

Rahman, M. S., Al-Marhubi, I. M., & Al-Mahrouqi, A. (2007). Measurement of glass transition temperature by mechanical (DMTA), thermal (DSC and MDSC), water diffusion and density methods: A comparison study. *Chemical Physics Letters*, *440*, 372–377.

Rieger, J. (2001). The glass transition temperature T_g of polymers – comparison of the values from differential thermal analysis (DTA DSC) and dynamic mechanical measurements (torsion pendulum). *Polymer Testing*, *20*, 199–204.

Robertson, C. G., & Palade, L. I. (2006). Unified application of the coupling model to segmental, Rouse, and terminal dynamics of entangled polymers. *Journal of Non-Crystalline Solids*, *352*, 342–348.

Robertson, C. G., & Rademacher, C. M. (2004). Coupling model interpretation of thermorheological complexity in polybutadienes with varied microstructure. *Macromolecules*, *37*, 10009–10017.

Roland, C. M., & Ngai, K. L. (1991). Segmental relaxation and molecular structure in polybutadienes and polyisoprene. *Macromolecules*, *24*, 5315–5319.

Schmidt, S. J. (2004). Water and solids mobility in foods. *Advances in Food and Nutrition Research*, *48*, 1–101.

Schmidt, S. J., Belton, P. S., Hills, B. P., & Webb, G. A. (1999). *Advances in magnetic resonance in food science*. Cambridge: The Royal Society of Chemistry.

Shivakumar, E., Das, C. K., Segal, E., & Narkis, M. (2005). Viscoelastic properties of ternary in situ elastomer composites based on fluorocarbon, acrylic elastomers and thermotropic liquid crystalline polymer blends. *Polymer*, *46*, 3363–3371.

Shrinivas, P., Kasapis, S., & Tongdang, T. (2009). Morphology and mechanical properties of bicontinuous gels of agarose and gelatin and the effect of added lipid phase. *Langmuir*, *25*, 8763–8773.

Tchesskaya, T. Y. (2005). Kinetics of semidilute and dense polymer solution: The time dependence of single-chain dynamics. *Journal of Molecular Liquids*, *120*, 143–146.

Tsui, N. T., Paraskos, A. J., Torun, L., Swager, T. M., & Thomas, E. L. (2006). Minimization of internal molecular free volume: A mechanism for the simultaneous enhancement of polymer stiffness, strength, and ductility. *Macromolecules*, *39*, 3350–3358.